Creating and controlling exceptional points of non-Hermitian Hamiltonians via homodyne Lindbladian invariance

Fabrizio Minganti [1,2,*] Dolf Huybrechts [3,†] Cyril Elouard,[4,‡] Franco Nori [5,6,7] and Ievgen I. Arkhipov [8,§]

[1]*Institute of Physics, Ecole Polytechnique Fédérale de Lausanne (EPFL), CH-1015 Lausanne, Switzerland*
[2]*Center for Quantum Science and Engineering, Ecole Polytechnique Fédérale de Lausanne (EPFL), CH-1015 Lausanne, Switzerland*
[3]*Univ Lyon, Ens de Lyon, CNRS, Laboratoire de Physique, F-69342 Lyon, France*
[4]*Inria, ENS Lyon, LIP, F-69342, Lyon Cedex 07, France*
[5]*Theoretical Quantum Physics Laboratory, RIKEN Cluster for Pioneering Research, Wako-shi, Saitama 351-0198, Japan*
[6]*RIKEN Center for Quantum Computing (RQC), Wako-shi, Saitama 351-0198, Japan*
[7]*Department of Physics, University of Michigan, Ann Arbor, Michigan 48109-1040, USA*
[8]*Joint Laboratory of Optics of Palacký University and Institute of Physics of CAS, Faculty of Science, Palacký University, 17. listopadu 12, 771 46 Olomouc, Czech Republic*

(Received 6 July 2022; accepted 19 September 2022; published 17 October 2022)

The exceptional points (EPs) of non-Hermitian Hamiltonians (NHHs) are spectral degeneracies associated with coalescing eigenvalues and eigenvectors, which are associated with remarkable dynamical properties. These EPs can be generated experimentally in open quantum systems, evolving under a Lindblad equation, by postselecting on trajectories that present no quantum jumps, such that the dynamics is ruled by a NHH. Interestingly, changing the way the information used for postselection is collected leads to different unravelings, i.e., different set of trajectories, which average to the same Lindblad equation, but are associated with a different NHH. Here, we exploit this mechanism to create and control EPs solely by changing the measurement we postselect on. Our scheme is based on a realistic homodyne reading of the emitted leaking photons with a weak-intensity laser (a process that we call β-dyne), which we show generates a tunable NHH, that can exhibit EPs even though the system does have any in the absence of the laser. We consider a few illustrative examples pointing out the dramatic effects that different postselections can have on the spectral features of the NHH, paving the road towards engineering of EPs in simple quantum systems.

DOI: 10.1103/PhysRevA.106.042210

I. INTRODUCTION

The study of exceptional points (EPs) is at the focus of intense experimental and theoretical research [1–3]. EPs are spectral singularities of non-Hermitian operators where both eigenvalues and eigenvectors coalesce [4], thus characterizing the dynamics of open quantum systems [5]. Such a singularity is mathematically associated with the nontrivial topological structure of the eigenvalue manifold, and the EP corresponds to a branching point of the solution of the characteristic polynomial of the corresponding non-Hermitian operator.

Beyond their theoretical and mathematical interest, EP's interest among physicists sparked from the discovery of parity-time ($\mathcal{PT}$) symmetry breaking, leading to the characterization of $\mathcal{PT}$ non-Hermitian Hamiltonians (NHHs) [6] and to the study of phase transitions in finite-dimensional systems [6,7]. Many experiments confirmed and demonstrated the unique properties of EPs and their influence on system dynamics, e.g., unidirectional invisibility [8,9], lasers with and enhanced-mode selectivity [10,11], low-power nonreciprocal light transmission [12,13], thresholdless phonon lasers [14,15], enhanced light-matter interactions [16–18], loss-induced lasing [19,20]. The nontrivial properties of the EPs have also been studied and analyzed in electronics [21], optomechanics [14,22,23], acoustics [24,25], plasmonics [26], and metamaterials [27]. At an EP, systems are also known for exhibiting nontrivial topological and localization properties, particularly in one-dimensional (1D) and higher-dimensional lattice architectures [1,28–43]. For extensive reviews see, e.g., Refs. [1,3,42,44] and references therein.

Many of the previously cited works dealt with semiclassical configurations, where the equation of motion of a strong coherent field can be mapped onto effective Schrödinger equations, leading to the appearance of Hamiltonian EPs (HEPs) [1,3,44,45]. When fully taking into account quantum dissipative processes, it is necessary to include the action of quantum jumps (Langevin noise), often significantly changing the dynamics of a quantum system [5,46–49]. To circumvent such a problem, and witness the EPs of a quantum NHH, two experimental strategies have been recently realized: dilation of a non-Hermitian Hamiltonian in a larger Hermitian space [50,51] and postselection [52,53]. In the latter case, EPs can be seen as one of the manifestations of the nontrivial dynamics of quantum systems under postselection [54,55].

*fabrizio.minganti@gmail.com
†dolf.huyb@gmail.com
‡cyril.elouard@gmail.com
§ievgen.arkhipov@upol.cz

 ©2022 American Physical Society

Indeed, under quite general hypotheses, the dynamics of open quantum systems can be described by a Lindblad master equation that, in turn, can be separated into the action of an effective NHH, periodically interrupted by abrupt events called quantum jumps [56,57]. According to this quantum trajectory picture, the Lindblad master equation is simply the description of the average dynamics of a system continuously probed by a set of detectors (modeling the environment), each one associated with a jump operator [58–60]. By postselecting those trajectories where no quantum jump occurs (no detector clicks), the spectral properties of the NHH can be investigated [52]. Within this postselected approach, the presence of EPs admits thus a simple and fascinating explanation: the very information gained by the fact that a quantum jump did not occur induces a nonunitary state update that, in turn, introduces the non-Hermiticity necessary to witness the wanted EP.

The formulation of quantum jumps, however, is not unique, and several quantum trajectory equations can be associated with the same Lindblad master equation [56,57,60]. Even if, usually, the quantum jumps and the NHH are represented in a standard form—the jump operators are chosen to be orthonormal and traceless—there exists a whole class of transformations, changing the effective Hamiltonian and the jump operators, which recover the same Lindblad master equation. However, the dynamics at a single trajectory level can drastically change according to the form of the effective Hamiltonian and of the jump operators stemming from these transformations [61–63]. The different forms of quantum trajectories, associated with a given Lindblad master equation, admit a clear physical interpretation and are called unraveling: they correspond to different ways to collect the information leaking from the system into the environment. Although the unconditional evolution (averaged over the detectors' output) is unchanged, these different monitorings modify the way the system behaves along single runs of an experiment, which are conditioned on a given sequence of detector outputs. This striking effect was experimentally demonstrated in, e.g., Ref. [64].

Since monitoring the occurrence of quantum jumps is the key ingredient for postselection, and the way the jump operators act modifies the non-Hermitian Hamiltonian, a natural question is what effects can be witnessed with these different unravelings of the same dissipative dynamics. In this paper, we demonstrate that different NHHs associated with the same Lindblad master equation display completely different spectral properties. In particular, by modifying the form of the quantum jumps (i.e., the way quantum information is collected) and postselecting those trajectories where no quantum jump occurred, we can induce an EP or modify its properties.

The paper is structured as follows. In Sec. II we introduce the Lindblad master equation and its invariances, leading to the different quantum trajectories associated with the same dynamics, as well as their postselection. We then introduce our first example in Sec. III, where we consider a two-level system (qubit) with gain and losses that does not display any EPs using the standard representation of the quantum jumps. However, tuning the previously introduced canonical transformations of the Lindblad master equation one can induce an EP. We then show in Sec. IV that it is possible to induce an EP in a driven Kerr resonator with a similar procedure, but just in the presence of photon loss. Finally, in Sec. V, we show that the canonical transformation can also be used to tune the properties of an EP. We present our conclusions in Sec. VI.

II. LINDBLAD INVARIANCES AND QUANTUM TRAJECTORIES

The state of an open quantum system is captured by its density matrix $\hat{\rho}(t)$. If the system interacts with a Markovian (memoryless) environment, and within the Born approximation, $\hat{\rho}(t)$ evolves under the Lindblad master equation, which reads [56,57]

$$\frac{\partial\hat{\rho}(t)}{\partial t} = \mathcal{L}\hat{\rho}(t) = -i[\hat{H},\hat{\rho}(t)] + \sum_{\mu}\gamma_{\mu}\mathcal{D}[\hat{J}_{\mu}]\hat{\rho}(t). \tag{1}$$

In this description, $\hat{H}$ is a Hermitian operator describing the coherent evolution of the system, while $\hat{J}_{\mu}$ are the jump operators describing the dissipation induced by the environment via the action of the dissipators, which reads

$$\mathcal{D}[\hat{J}_{\mu}]\hat{\rho}(t) = \hat{J}_{\mu}\hat{\rho}(t)\hat{J}_{\mu}^{\dagger} - \frac{\hat{J}_{\mu}^{\dagger}\hat{J}_{\mu}\hat{\rho}(t) + \hat{\rho}(t)\hat{J}_{\mu}^{\dagger}\hat{J}_{\mu}}{2}. \tag{2}$$

A. Quantum trajectories

From a theoretical point of view, the Lindblad master equation is a particular form of a quantum map [65]. On a general ground, any quantum map can be rewritten in terms of its Kraus operators, and

$$\hat{\rho}(t+dt) = \sum_{\nu}\hat{K}_{\nu}\hat{\rho}(t)\hat{K}_{\nu}^{\dagger}, \tag{3}$$

where the condition

$$\sum_{\nu}\hat{K}_{\nu}^{\dagger}\hat{K}_{\nu} = \hat{\mathbb{1}} \tag{4}$$

is required to ensure that the quantum map is completely positive and trace preserving (CPTP). Given the form of Eq. (1), one can verify that a set of Kraus operators that recover the Lindblad master equation is

$$\begin{aligned}\hat{K}_0 &= \hat{\mathbb{1}} - i\hat{H}dt - \sum_{\mu}\gamma_{\mu}\frac{\hat{J}_{\mu}^{\dagger}\hat{J}_{\mu}}{2}dt = \hat{\mathbb{1}} - i\hat{H}_{\text{eff}}dt,\\ \hat{K}_{\nu} &= \sqrt{\gamma_{\mu}dt}\hat{J}_{\nu},\end{aligned} \tag{5}$$

where the non-Hermitian Hamiltonian (NHH) $\hat{H}_{\text{eff}}$ is

$$\hat{H}_{\text{eff}} = \hat{H} - i\sum_{\mu}\gamma_{\mu}\frac{\hat{J}_{\mu}^{\dagger}\hat{J}_{\mu}}{2}. \tag{6}$$

Each Kraus operator can be associated with one of the possible outcomes of a measurement process, whose backaction on the system is associated with the $\hat{K}_{\nu}$ operator. In this regard, the Lindblad master equation can be interpreted as the dynamics of a system upon the continuous action of several measurement instruments. Whenever the outcome $\nu \neq 0$ is obtained at time t, one of the detectors clicks and the system evolves under the action of $\hat{K}_{\nu}$. If none of the detectors click, the system evolves according to $\hat{K}_0$, as the absence of clicks still conveys some information about the system state

[60], yielding Eq. (3) when the average over the measurement outcomes is taken.

From this interpretation it is natural to introduce quantum trajectories. By keeping track of the measurement outcomes (the sequence of quantum jumps), we can exactly reconstruct the state of a given system initialized in a pure state $|\Psi(t=0)\rangle$ [65]. If the $\hat{K}_0$ acts, the time (unnormalized) evolution of the system is described by

$$\partial_t|\Psi(t)\rangle = -i\hat{H}_{\text{eff}}|\Psi(t)\rangle, \tag{7}$$

while, if the νth Kraus operator acts, the system evolves as

$$|\Psi(t+dt)\rangle \propto \hat{J}_\nu|\Psi(t)\rangle. \tag{8}$$

If we consider the dynamics where no quantum jumps occur, the system evolves solely under the action of the NHH $\hat{H}_{\text{eff}}$. Thus, a postselection on those trajectories with no quantum jumps reveals the spectral properties of the NHH $\hat{H}_{\text{eff}}$ in Eq. (6). In particular, we can define the eigenvectors $|\Psi_j\rangle$ and the associated eigenenergies E_j such that

$$\hat{H}_{\text{eff}}|\Psi_j\rangle = E_j|\Psi_j\rangle. \tag{9}$$

An EP of the NHH is then defined as a point where $E_j = E_k$ and $|\Psi_j\rangle = |\Psi_k\rangle$. Higher-order degeneracies can take place, and for this reason one calls the order of an EP the number of coalescing eigenvectors (e.g., $|\Psi_j\rangle = |\Psi_k\rangle = |\Psi_l\rangle$ is an EP of order 3).

As it has been experimentally shown in Ref. [52], this postselection procedure allows studying the emergence of the Hamiltonian EPs, i.e., the degeneracy of the NHH, by reconstructing the evolution of the quantum system. In principle, one needs perfect detectors that detect the jumps with unitary efficiency and exhibit no dark counts. In the presence of finite-efficiency detectors, however, one can still observe the effects of the EP of NHH by analyzing the associated hybrid Liouvillian [49].

Notice that, just as for any quantum dynamics, in order to experimentally assess the properties of a system evolving at an EP, it is not sufficient to just know that no jump occurred. Indeed, the simple measurement of the jump operators does not not yield all the information about the system state, allowing us to completely characterize the properties of the system. For instance, in a qubit system, determining the presence of an EP amounts to (i) postselect the trajectory where no jump happened; (ii) perform a measurement of the system at a given time t; (iii) repeat the measurement for different runs (having initialized the system in the same state); (iv) repeat the same procedure for several different times t. This procedure highlights the presence of an anomalous dynamics associated with an EP.

B. Lindbladian invariances, measurements, and new trajectories

Jump operators are usually chosen to be traceless ($\text{Tr}[\hat{J}_\mu] = 0$) and orthonormal ($\text{Tr}[\hat{J}_\mu\hat{J}_\nu] \propto \delta_{\mu\nu}$). Such a choice, although mathematically convenient, should not be privileged from a physical point of view. Indeed, the set of jump operators associated with a given Lindblad equation is not uniquely determined.

Consider, for instance, the affine transformations

$$\begin{aligned}\hat{J}'_\mu &= \hat{J}_\mu + \beta_\mu\hat{\mathbb{1}},\\ \hat{H}' &= \hat{H} - \sum_\mu \frac{i\gamma_\mu}{2}(\beta^*_\mu\hat{J}_\mu - \beta_\mu\hat{J}^\dagger_\mu).\end{aligned} \tag{10}$$

Although Eq. (10) modifies both the Hamiltonian and the jump operators, it does not change the Lindblad master equation result. Indeed, one can easy show that, the Lindblad master equation stemming from $\hat{H}'$ and $\hat{J}'_\mu$ is the same as Eq. (1) [56]. However, for $\beta \neq 0$, the effective Hamiltonian changes as

$$\begin{aligned}\hat{H}_{\text{eff}}(\beta) = \hat{H} &- \sum_\mu \frac{i\gamma_\mu}{2}(\beta^*_\mu\hat{J}_\mu - \beta_\mu\hat{J}^\dagger_\mu)\\ &- \sum_\mu \frac{i\gamma_\mu}{2}(\hat{J}_\mu + \beta_\mu\hat{\mathbb{1}})^\dagger(\hat{J}_\mu + \beta_\mu\hat{\mathbb{1}}).\end{aligned} \tag{11}$$

In quantum optics, the quantum trajectory stemming from the orthonormal set $\hat{J}_\nu \equiv \hat{a}(\omega)$ [where $\hat{a}(\omega)$ is the annihilation operator of the mode at frequency ω] describes a situation in which the photons emitted by the system are instantaneously detected by a photon counter, while the set of jumps $\hat{J}'_\nu$, defined by Eq. (10), is relevant in the case of a homodyne detection setup. In the latter case, the emitted photons are mixed with a coherent field on a beam splitter before being detected. For usual homodyne detection, one chooses $|\beta|^2 \gg 1$, while here we will consider finite values of β (associated with a weaker coherent field). For this reason we call such a trajectory resulting from Eq. (10) and from Eq. (11) a β-dyne unraveling (see also Appendixes A and B for a theoretical model of this detection setup, its physical interpretation, and the derivation of the associated dynamics).

It is rather remarkable that the affine transformation in Eq. (10) produces an ambiguity in the realization of the system's quantum trajectories. For instance, consider again a bosonic system characterized, this time, by just one annihilation operator $\hat{J}_\nu = \hat{a}$ (i.e., the environment induces dissipation in the form of particle losses described by $\mathcal{D}[\hat{a}]$ in the average dynamics). The effect of the β-dyne unraveling at a single trajectory level is that (i) the action of the jump operators $\hat{J}'_\nu$ do not eject one full photon from the system and (ii) when the jump $\hat{J}'_\nu$ does not occur the bosonic field within the cavity gets displaced by a coherent amplitude $\gamma_\mu\beta/2$, according to Eq. (10). What are then the effects of this invariance on the spectral properties of the non-Hermitian Hamiltonian, and can they be detected experimentally? That is, can one practically implement a postselection procedure that, even if the average dynamics is purely incoherent, exhibits a significantly different dynamics at the NHH level? Below, we show that the transformation Eq. (10) can profoundly change the structure of the NHH, even inducing the presence of EPs in otherwise nondegenerate Hamiltonians. Owing to the postselected measurement, we prepared the system at an EP, and the standard measurement protocol on the system, i.e., the points (i)–(iv) described in Sec. II A, can demonstrate the properties of the system.

Even if in the following, we will focus on the β-dyne transformation induced by Eq. (10), for the sake of completeness let us notice that not all transformations on the Lindblad mas-

ter equation modify the structure of the NHH. For instance, the unitary transformation

$$\sqrt{\gamma'_\mu}\hat{J}'_\mu = \sum_\nu R_{\mu,\nu}\sqrt{\gamma_\nu}\hat{J}_\nu \tag{12}$$

leaves both the Lindlbad master equation and the NHH unchanged if $R_{\mu,\nu}$ is a unitary matrix. Indeed,

$$\begin{aligned}\hat{H}'_{\text{eff}} &= \hat{H} - \sum_\mu \frac{i\gamma'_\mu}{2}\hat{J}'^\dagger_\mu \hat{J}'_\mu \\ &= \hat{H} - \sum_{\mu,\nu,\chi} R^*_{\mu,\nu}R_{\mu,\chi}\frac{i\sqrt{\gamma_\nu\gamma_\chi}}{2}\hat{J}^\dagger_\nu\hat{J}_\chi \\ &= \hat{H} - \frac{i}{2}\sum_\mu \gamma_\mu \hat{J}^\dagger_\mu\hat{J}_\mu = \hat{H}_{\text{eff}},\end{aligned} \tag{13}$$

because $R_{\mu,\nu}$ is unitary, i.e., $\sum_\mu R^*_{\mu,\nu}R_{\mu,\chi} = \delta_{\nu,\chi}$. Thus, if we mix the leaking fields, all postselected dynamics result in the same NHH.

III. EXAMPLE I: INDUCING AN EP BY POSTSELECTION OF A β-DYNE TRAJECTORY

As a starting point for our discussion, let us consider a two-level system, whose most general NHH reads

$$\begin{pmatrix} a & b \\ c & d\end{pmatrix} = \begin{pmatrix} \tilde{a} & b \\ c & 0\end{pmatrix} + d\begin{pmatrix} 1 & 0 \\ 0 & 1\end{pmatrix}, \tag{14}$$

where $\tilde{a} = a - d$. The eigenvalues read

$$\frac{2d + \tilde{a} \pm \sqrt{\tilde{a}^2 + 4bc}}{2}, \tag{15}$$

and the (unnormalized) eigenvectors are

$$\{\tilde{a} \pm \sqrt{\tilde{a}^2 + 4bc},\ 2c\}. \tag{16}$$

Consequently, the condition to observe an EP in a two-level system can be recast as

$$\tilde{a} = \pm 2i\sqrt{bc}. \tag{17}$$

A. EP of a qubit with loss and gain

Consider a two-level system whose Hamiltonian is

$$\hat{H} = \frac{\omega}{2}\hat{\sigma}_z, \tag{18}$$

and with jump operators

$$\hat{J}_1 = \sqrt{\gamma}_-\hat{\sigma}_-, \quad \hat{J}_2 = \sqrt{\gamma}_+\hat{\sigma}_+, \tag{19}$$

where $\hat{\sigma}_z$ is the z Pauli matrix and $\hat{\sigma}_\pm$ are the raising and lowering qubit operators, respectively. If we monitor the jump operator $\hat{J}_1$, then the effective Hamiltonian of this system is

$$\hat{H}_{\text{eff}} = \frac{1}{2}\begin{pmatrix} \omega - i\gamma_- & 0 \\ 0 & -\omega - i\gamma_+\end{pmatrix}. \tag{20}$$

Consequently, this model can never display any exceptional point, because the eigenvalues are always distinct and separated.

Let us now consider the β-dyne detection of both the jump operators with the same intensity β, via the transformation

$$\hat{J}'_1 = \sqrt{\gamma}_-(\hat{\sigma}_- + \beta\hat{\mathbb{1}}), \quad \hat{J}'_2 = \sqrt{\gamma}_+(\hat{\sigma}_+ + \beta\hat{\mathbb{1}}). \tag{21}$$

The corresponding effective Hamiltonian is

$$\begin{aligned}\hat{H}_{\text{eff}}(\beta) = &-i\frac{|\beta|^2(\gamma_- + \gamma_+)}{2}\hat{\mathbb{1}} \\ &+ \frac{1}{2}\begin{pmatrix} \omega - i\gamma_- & -2i\beta^*\gamma_+ \\ -2i\beta^*\gamma_- & -\omega - i\gamma_+\end{pmatrix}.\end{aligned} \tag{22}$$

The NHH $\hat{H}_{\text{eff}}$ has now the right structure to display an EP. In particular, the eigenvalues and eigenvectors read

$$E_{1,2} = -i\frac{\gamma_- + \gamma_+ + 2|\beta|^2(\gamma_- + \gamma_+) \pm \sqrt{16\gamma_-\gamma_+(\beta^*)^2 + (\gamma_- - \gamma_+ + 2i\omega)^2}}{4}. \tag{23}$$

$$|\Psi_{1,2}\rangle = \frac{1}{\sqrt{\mathcal{N}_{1,2}}}\{2i\omega\gamma_- - \gamma_+ \pm \sqrt{16\gamma_-\gamma_+(\beta^*)^2 + (\gamma_- - \gamma_+ + 2i\omega)^2}, 4\gamma_-\beta^*\}, \tag{24}$$

where $\mathcal{N}_{1,2}$ is a a normalization factor ensuring $\langle\Psi_{1,2}|\Psi_{1,2}\rangle = 1$. The EP emerges when

$$\beta = \pm i\frac{\gamma_- - \gamma_+ - 2i\omega}{4\sqrt{\gamma_-\gamma_+}}. \tag{25}$$

We show the effect of β in Fig. 1, where we plot the overlap between the two eigenvectors of $\hat{H}_{\text{eff}}(\beta)$. In general, the presence of an EP implies the coalescence of (at least) the eigenvectors of a non-Hermitian Hamiltonian. Thus, the overlap $\langle\Psi_1|\Psi_2\rangle$ between two normalized vectors indicates how close a system is to an EP, reaching 1 exactly at the EP. In particular, we notice that there is a whole region around the β_{EP} value where the eigenvectors almost coalesce, showing the dramatic effect that the introduction of β can induce on the spectral properties of the NHH. In Fig. 2, instead, we show the emergence of the EP as a function of γ_+/γ_-, having fixed the value of β. Compared to the $\beta = 0$ case in Fig. 2(a), we remark that the eigenfrequencies now change both in real and imaginary parts as a function of γ_+.

B. Physical realization

Despite its relative algebraic simplicity, the previous examples require the simultaneous postselection of both the jumps occurring from $\hat{\sigma}^-$ and $\hat{\sigma}^+$. While the former implies a spontaneous emission that can be, in principle, achieved via a high-fidelity detector, the latter corresponds to spontaneous excitation through gaining mechanisms, and its detection can be remarkably more difficult. Such a proof-of-concept model can be realized, however, by using a three-level system instead of a qubit [66,67].

Consider a three-level system, whose undriven energy eigenstates $|g\rangle$, $|e\rangle$, and $|f\rangle$ are coupled by a weak coherent

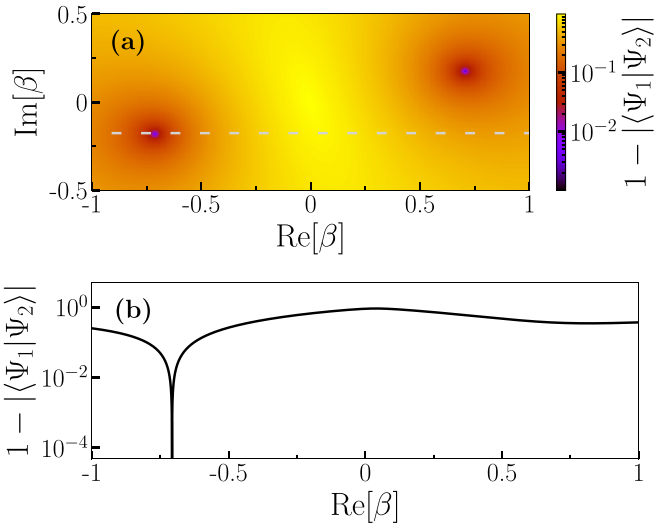

FIG. 1. The overlap between the two normalized eigenvectors $|\Psi_{1,2}\rangle$ of the NHH in Eq. (24) as a function of β, having fixed $\gamma_+ = 0.5\gamma_-$ and $\omega = \gamma_-$. (a) The contour plot in the real and imaginary part of β shows that, by appropriately choosing the value of β, it is possible to make $|\Psi_{1,2}\rangle$ coalesce. (b) Overlap along the gray dashed line in panel (a), showing the abrupt change in the orthogonality properties of the eigenvectors near the EP.

drive resonant with the transition between states $|g\rangle$ and $|f\rangle$ (cf. Fig. 3), according to the Hamiltonian

$$\hat{H}(t) = |e\rangle\langle e| + (2\omega + \delta\omega)|f\rangle\langle f| + \Omega(|g\rangle\langle f|e^{i\omega_{ef}t} + |f\rangle\langle g|e^{-i\omega_{ef}t}). \quad (26)$$

The spontaneous emission of photons induces the decay of level $|f\rangle$ to $|e\rangle$, and from level $|e\rangle$ to the ground state $|g\rangle$, via

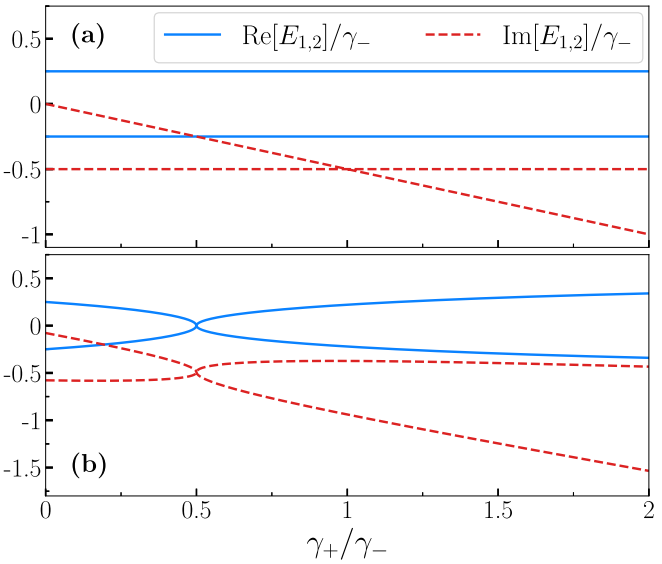

FIG. 2. Real (blue solid curve) and imaginary (red dashed curve) parts of the two eigenvalues of the NHH in Eqs. (23) and (24) as a function of the gain over loss ratio γ_+/γ_-. (a) When $\beta = 0$, the system does not exhibit an EP. (b) For nonzero $\beta \neq 0$, an EP emerges the system [in this specific case $\beta = (2+i)/4\sqrt{2}$]. We fix $\omega = \gamma_-$.

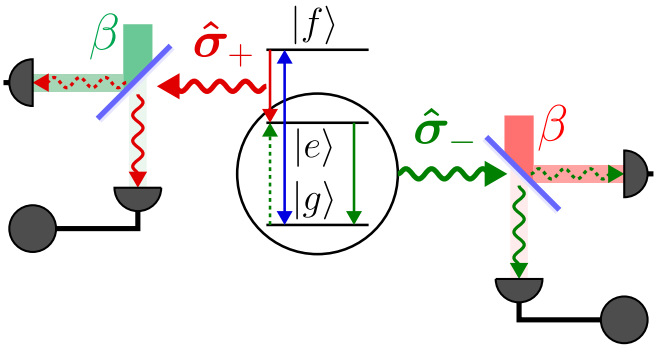

FIG. 3. Setup to perform the β-dyne detection of a qubit with effective gain and saturation, leading to Eq. (22). A three-level system, characterized by the states $|g\rangle$, $|e\rangle$ (at energy ω), and $|f\rangle$ (at energy $2\omega + \delta\omega$), is subject to decays $|e\rangle \to |g\rangle$ (green solid arrow) and $|f\rangle \to |e\rangle$ (red arrow) at rates $\gamma_{eg} \ll \gamma_{fe}$. A weak drive coherently couples the state $|g\rangle$ and $|f\rangle$ (blue arrow). The decay γ_{eg}, characterized by a jump operator $\hat{\sigma}_-$, is associated with the emission of an photon with energy ω, and can be detected via the standard homodyne detection leading to Eq. (10). The overall effect of the process $|g\rangle \to |f\rangle \to |e\rangle$ is, instead, to induce an effective gain $|g\rangle \to |e\rangle$ (dashed green arrow) associated to the jump operator $\hat{\sigma}_+$, because of the rapid decay of $|f\rangle$. Such a gain, however, is accompanied by the emission of a photon with energy $\omega + \delta$, on which one can perform standard homodyne detection and postselection.

the Lindbladian:

$$\mathcal{L}_1 = \gamma_{eg}\mathcal{D}[|g\rangle\langle e|] + \gamma_{fe}\mathcal{D}[|e\rangle\langle f|]. \quad (27)$$

If we assume that $\gamma_{fe} \gg \gamma_{eg}, \Omega$, we can adiabatically eliminate the state $|f\rangle$. The combined action of the driving and the dissipation results in a new Lindbladian

$$\mathcal{L}_2 = \gamma_{eg}\mathcal{D}[|g\rangle\langle e|] + \gamma_{\rm eff}\mathcal{D}[|e\rangle\langle g|], \quad (28)$$

which therefore implements the wanted model with $\gamma_+ \equiv \gamma_{\rm eff} = 4\Omega^2/\gamma_{fe}$ and $\gamma_- \equiv \gamma_{eg}$. Notice that a jump from state $|g\rangle$ to $|e\rangle$ is associated with the emission of a photon at the frequency $(\omega + \delta\omega)$, which can thus be detected with a photon counter. Such a jump can be distinguished from the one associated with $|g\rangle \to |e\rangle$, because the latter leads to the emission of a photon at frequency ω.

IV. EXAMPLE II: INDUCING AN EP IN THE DRIVEN KERR RESONATOR

In this section, we present a protocol based on a driven-dissipative Kerr resonator (see Fig. 4), which requires detection of only emitted photons (i.e., the detection of one jump operator) in order to reveal the emergence of EPs in the postselected effective Hamiltonians.

The Hamiltonian of a Kerr resonator, in the frame rotating at the drive frequency, is

$$H = -\Delta\hat{a}^\dagger\hat{a} + U\hat{a}^{\dagger 2}\hat{a}^2 - i(\alpha\hat{a}^\dagger - \alpha^*\hat{a}), \quad (29)$$

where $\hat{a}$ ($\hat{a}^\dagger$) is an annihilation (creation) field operator, Δ is the pump-to-cavity detuning, U is a Kerr nonlinearity, α is the amplitude of the coherent field, which drives the resonator. We assume that the system is subject to one-photon loss events described by the dissipator $\mathcal{D}[\hat{a}]$, occurring at a rate γ.

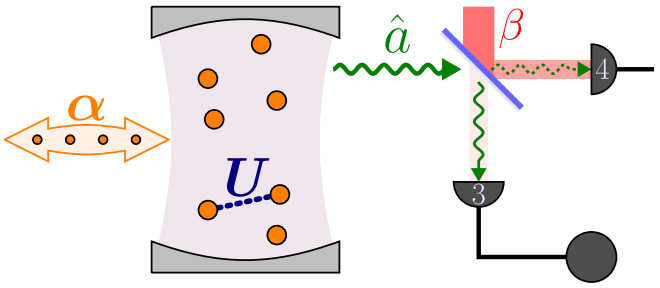

FIG. 4. Setup to perform the β-dyne detection of a driven Kerr resonator, described by Eq. (30). The Kerr resonator is driven by a field of intensity α, and two photons interact within the cavity with an intensity U. The emitted photons ($\hat{a}$ in green) are then mixed with a field whose effective intensity is β, as detailed in Eq. (10).

Let us now assume that the system is at resonance, $\Delta = 0$, and it is postselected in a β-dyne picture; thus, the NHHs $\hat{H}_{\rm eff}(\beta)$ is coherently displaced by the amplitude β, according to Eq. (11). Assuming the weak-driving limit, i.e., $\alpha \ll \gamma, U$, and assuming also that $\beta \ll \gamma$, one can write down the effective Hamiltonian in the two-photon limit (i.e., truncating the Fock space at two photons), resulting in a three-level system that reads

$$H_{\rm eff} = \begin{pmatrix} 0 & i\alpha^* - i\gamma\beta^* & 0 \\ -i\alpha & -\frac{i}{2}\gamma & i\sqrt{2}(\alpha^* - \gamma\beta^*) \\ 0 & -i\sqrt{2}\alpha & -i\gamma + 2U \end{pmatrix} - \frac{i\gamma|\beta|^2}{2}\mathbb{I}_3. \tag{30}$$

If $\beta = 0$, no combination of parameters of the NHH results in an EP. In other words, whenever one is monitoring the system's environment and leaked photons are not displaced by a coherent field, then the corresponding postselected NHH

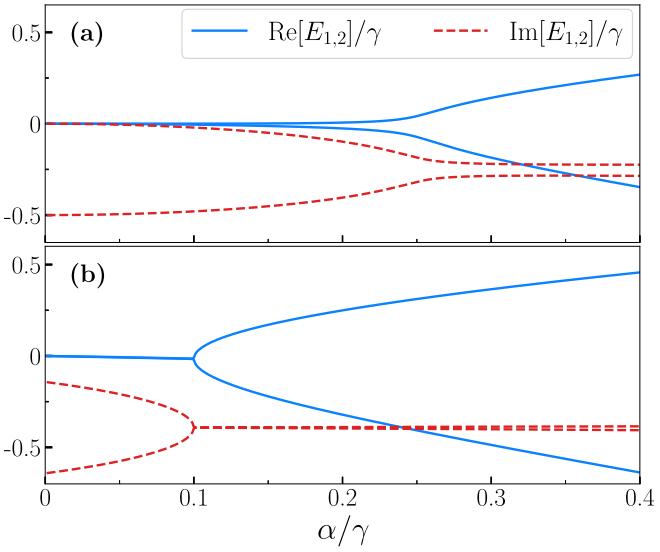

FIG. 5. Real (blue solid curve) and imaginary (red dashed curve) parts of the two eigenvalues of the NHH in Eq. (30) as a function of (purely) real-valued α. (a) When $\beta = 0$, the system does not exhibit an EP. (b) At certain nonzero $\beta \neq 0$, an EP may be induced in the system (in this specific case $\beta = -0.5275 - 0.078i$). The rest of the system parameters are $\gamma = 1$, $U = 2$.

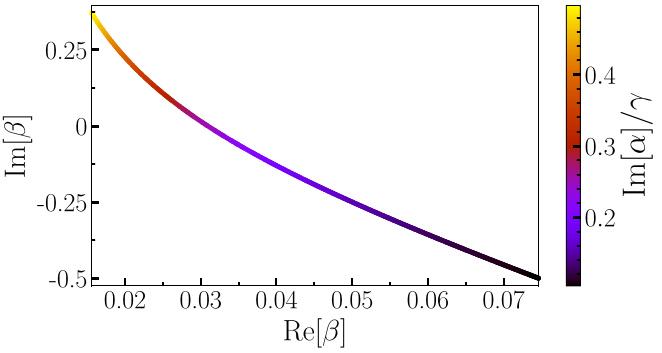

FIG. 6. Values for the real and imaginary parts of the displaced field β, for a given purely imaginary-valued α, at which the NHH $\hat{H}_{\rm eff}(\beta)$ can exhibit an EP, according to Eq. (31). Other parameters are as in Fig. 5.

$\hat{H}_{\rm eff}(\beta = 0)$ does not have any spectral singularity [see, e.g., Fig. 5(a)].

For $\beta \neq 0$, instead, the condition for the NHH to have an EP of the second order reads:

$$\begin{aligned} &a^2 - 3b - 9ab + 27c + 2a^3 - 3\sqrt{3} \\ &\quad \times [27c^2 + (4a^3 - 18ab)c - a^2b^2 + 4b^3]^{\frac{2}{3}} \\ &\quad = 0, \end{aligned} \tag{31}$$

where

$$a = \frac{3i\gamma}{2} - 2U,\ b = 3\alpha\beta^*\gamma - 3|\alpha|^2 - \frac{1}{2}\gamma^2 - iU\gamma,$$
$$c = (i\gamma - 2U)(\gamma\beta^*\alpha - |\alpha|^2).$$

Having fixed the system parameters, these equations can be numerically solved to find the values of β resulting in an EP (see Fig. 6). Note that only a second-order EP can be observed in the $\hat{H}_{\rm eff}(\beta)$, since at most only two of the three eigenvalues of the NHH coincide.

We conclude that, if one postselects those experiments where the detector never clicks, and for an appropriate choice of β, satisfying the condition in Eq. (31), then the effective Hamiltonian in Eq. (30) exhibits a second-order EP in the system [see Fig. 5(b)]. We stress that the full Lindbladian of the system does not have a Liouvillian EP, in the sense described in Ref. [5]. Indeed, the Linbladian describes the dynamics of the operator averages and, as such, its averaging over various quantum trajectories eventually smears out EPs, which emerge in certain effective NHHs. The presence of an EP in the NHH is thus an effect that can only really emerge at the single-trajectory level.

V. EXAMPLE III: SHIFTING AN EP

The effect of β is not only to generate new EPs in a quantum system; adjusting β also allows one to shift the position and change the nature (i.e., the associated eigenvalues and eigenvectors) of an existing EP.

Consider a resonantly driven two-level system as in Fig. 7, whose Hamiltonian in the pump frame reads

$$\hat{H} = \frac{\omega}{2}\hat{\sigma}_x. \tag{32}$$

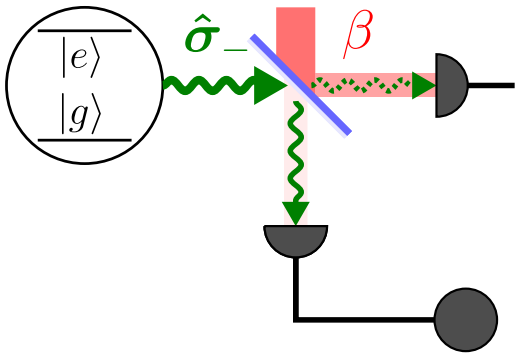

FIG. 7. Setup to perform β-dyne detection of a driven qubit, described by Eq. (35). The qubit is driven by a field at resonance. The emitted photons are then mixed with a field whose effective intensity is β, as detailed in Eq. (10).

Let us assume that the system is affected by a dissipation channel $\gamma_-\mathcal{D}[\hat{\sigma}_-]$. The effective non-Hermitian Hamiltonian of such a system in the standard representation is given by

$$\hat{H}_{\rm eff} = \frac{1}{2}\begin{pmatrix} -i\gamma_- & \omega \\ \omega & 0 \end{pmatrix}, \tag{33}$$

which exhibits an exceptional point for

$$\omega = \frac{\gamma_-}{2}. \tag{34}$$

We now assume that the emitted photons are detected via the β-dyne scheme. The associated non-Hermitian Hamiltonian is:

$$\hat{H}_{\rm eff}(\beta) = -i\frac{|\beta|^2\gamma_-}{2}\hat{\mathbb{1}} + \frac{1}{2}\begin{pmatrix} -i\gamma_- & \omega \\ \omega - 2i\beta^*\gamma_- & 0 \end{pmatrix}, \tag{35}$$

whose eigenvalues are

$$E_{1,2} = \frac{-i\gamma_- + 2i|\beta|^2\gamma_- \pm \sqrt{-\gamma_-^2 + 4\omega^2 + 8i\gamma_-\omega\beta^*}}{4}, \tag{36}$$

and the normalized eigenvectors ($\mathcal{N}_{1,2}$ ensures $\langle\Psi_{1,2}|\Psi_{1,2}\rangle = 1$)

$$|\Psi_{1,2}\rangle = \frac{1}{\sqrt{\mathcal{N}_{1,2}}}\{-i\gamma_- \pm \sqrt{-\gamma_-^2 + 4\omega^2 + 8i\gamma_-\omega\beta^*}, 2(\omega + 2i\beta^*\gamma_-)\}. \tag{37}$$

The exceptional point is now determined at

$$\beta = i\frac{4\omega^2 - \gamma_-^2}{8\gamma_-\omega}. \tag{38}$$

For $\beta = 0$ we retrieve Eq. (34); for different values of β, the EP position, eigenvalues, and eigenvectors change. We show this effect in Figs. 8 and 9. We find that an EP can be always found having fixed ω/γ_- [Figs. 9(a) and 9(b)], and that, for an imaginary-valued β, the value ω/γ_- for which an EP emerges strongly depends on β. Notice that the shift of the EP comes at the expense of a decreased no-jump trajectory probability. A detailed computation of the postselection probability is reported in Appendix B.

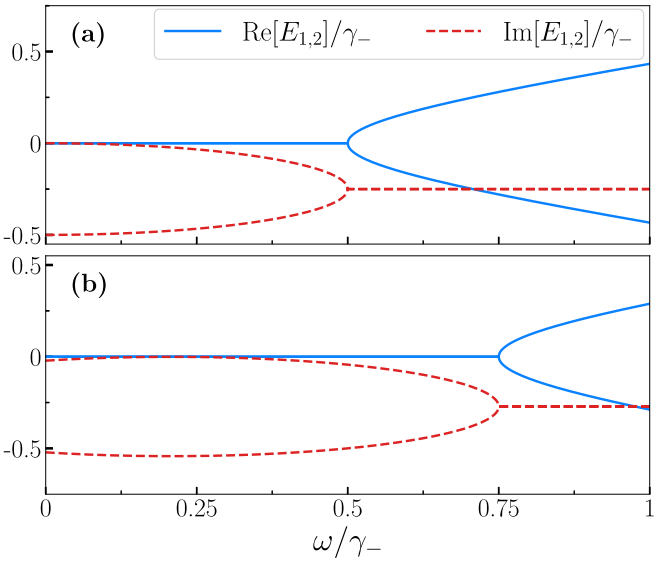

FIG. 8. (a) $\beta = 0$ with an exceptional point at $\omega = \frac{1}{2}\gamma_-$ and (b) $\beta = \frac{5}{24}i$ with an exceptional point at $\omega = \frac{3}{4}\gamma_-$.

A final comment is necessary. As we already discussed, the postselection procedure of the Lindblad master equation can be, in principle, associated with different types of unraveling. There are myriads of possible trajectories, including those with various values of β, inducing different coherent displacements [due to the Lindbladian invariance in Eq. (10)]. This illustrates the fundamental difference between Liouvillian and Hamiltonian EPs. Liouvillian EPs exist at the level of the average dynamics of an open quantum system, and appear independently of the specific characteristics of the system-environment coupling. The EPs of a NHH, which are induced by postselection, appear only for specific types of jump operators. Furthermore, the fact that EPs of an NHH can be shifted by different unraveling via the action of β is also a signature of the relative fragility of the EPs of postselected NHHs. Indeed, both the system's parameters and those of the detector, whose action determines the effect of the postselection procedure, must be finely tuned.

VI. CONCLUSION

By exploiting homodyne Lindbladian invariance, i.e., by displacing the emitted leaking photons with a laser field and keeping the whole Lindbladian unchanged, we show that one

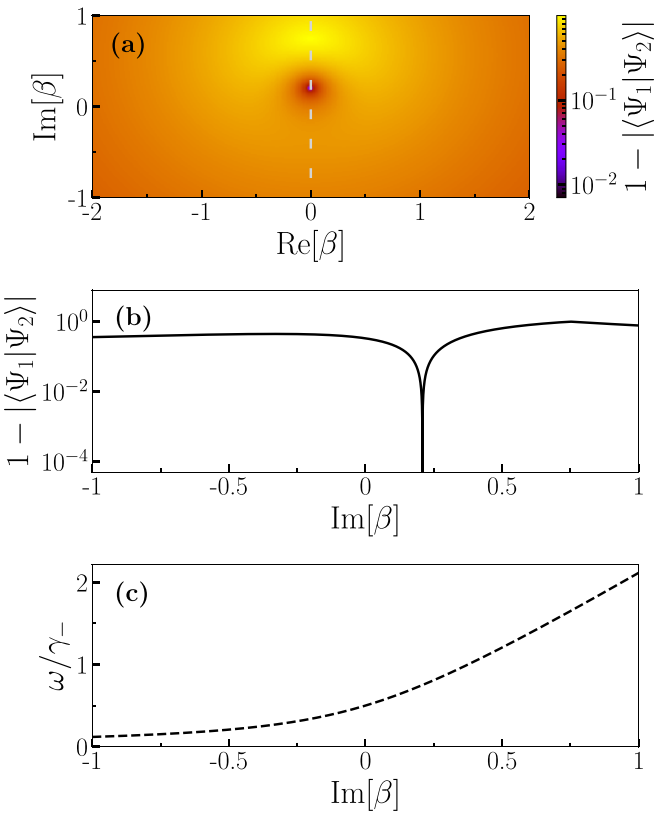

FIG. 9. The overlap between the two normalized eigenvectors $|\Psi_{1,2}\rangle$ of the NHH in Eq. (37) as a function of β, having fixed $\omega = \frac{3}{4}\gamma_-$. (a) The contour plot in the real and imaginary part of β shows that, by appropriately choosing the value of β, it is possible to make $|\Psi_{1,2}\rangle$ coalesce. (b) Overlap along the gray dashed line in (a), showing the abrupt change in the orthogonality properties of the eigenvectors near the EP. (c) Position of the EP in rescaled frequency ω/γ_- as a function of the β parameter obtained from Eq. (38). To ensure the presence of an EP, β is chosen purely imaginary.

can end up with different forms of quantum trajectories. Under postselection of no-jump trajectories, this scheme generates dynamics generated by a non-Hermitian Hamiltonian (NHH) whose spectral properties can be tuned via the parameters of the laser field used for the displacement. We illustrate the potential of this scheme on three examples based on simple quantum systems and realistic detection setups, where exceptional points (EPs) can be generated or controlled only by changing the displacement of the leaking photons. This control on the EP, however, comes at the price of a more stringent postselection, decreasing the probability of occurrence of the no-jump trajectory. More generally, our approach exploits the mathematical invariance of the Lindblad equation to provide a whole toolbox to engineer EP properties, opening the perspectives of new implementations of EP and their predicted applications, e.g., in metrology [17,18] or optimal energy transfer [22,68,69].

ACKNOWLEDGMENTS

F.M. thanks the Laboratoire de physique in the ENS of Lyon, and Prof. Tommaso Roscilde, for the hospitality. D.H. acknowledges support from QuantERA ("MAQS" project). F.N. is supported in part by: Nippon Telegraph and Telephone Corporation (NTT) Research, the Japan Science and Technology Agency (JST) [via the Quantum Leap Flagship Program (Q-LEAP) program, and the Moonshot R&D Grant No. JPMJMS2061], the Japan Society for the Promotion of Science (JSPS) [via the Grants-in-Aid for Scientific Research (KAKENHI) Grant No. JP20H00134], the Army Research Office (ARO) (Grant No. W911NF-18-1-0358), the Asian Office of Aerospace Research and Development (AOARD) (via Grant No. FA2386-20-1- 4069), and the Foundational Questions Institute Fund (FQXi) via Grant No. FQXi-IAF19-06. I.A. thanks the Project No. CZ.02.1.01/0.0/0.0/16_019/0000754 of the Ministry of Education, Youth and Sports of the Czech Republic.

APPENDIX A: IMPLEMENTATION OF THE β-DYNE MEASUREMENT SETUP AND PHYSICAL INTERPRETATION OF EQ. (10)

The β-dyne measurement scheme is not only a mathematical object but can actually be implemented experimentally. It corresponds to a variation of the commonly used homodyne measurement protocol in quantum optics [65]. In such setup, the signal (field emitted by the system) is mixed with an intense coherent field on an unbalanced beam splitter with very low reflectance $\eta \ll 1$. The transmitted signal is then measured with a photon counter (see also the scheme in Fig. 4).

The annihilation operators at the output ports 3,4 of the beam splitter are related to the input 1,2 via:

$$\hat{a}_3 = \sqrt{1-\eta}\,\hat{a}_1 + \sqrt{\eta}\,\hat{a}_2 \tag{A1}$$

$$\hat{a}_4 = -\sqrt{\eta}\,\hat{a}_1 + \sqrt{1-\eta}\,\hat{a}_2. \tag{A2}$$

For $\eta \ll 1$ and mode $\hat{a}_2$ prepared in a coherent state of amplitude $|\alpha_2| \gg 1$, we can see that the field at port 3 is approximately described by

$$\hat{a}_3 \simeq \hat{a}_1 + \sqrt{\eta}\alpha_2. \tag{A3}$$

Finally, as field $\hat{a}_1$ is populated by the system's emission, the detection of a click at port 3 therefore corresponds effectively to a jump of the system, captured by a coherently displaced jump operator of the form $\hat{a} + \beta\hat{\mathbb{1}}$. Consequently, everything happens as if the β-dyne measurement effectively generated a virtual field driving the system. This dynamics, including the effect of the virtual field, can be experimentally demonstrated; e.g., from multiple repetitions of the β-dyne measurement starting in the same state, followed by a projective measurement on the system. Below, we derive more rigorously the backaction of such measurement on the system so as to deduce the postselection probability for the β-dyne no-jump trajectory.

APPENDIX B: β-DYNE MEASUREMENT SETUP: THEORETICAL MODEL FOR THE BACKACTION AND POSTSELECTION PROBABILITY

To demonstrate the setup able to implement the β-dyne measurement we discuss throughout the paper, we now consider an emitter with Hamiltonian $\hat{H}_S$, whose light emission is collected into the port 1 of a beam splitter. Port 2 corresponds to the incoming laser, which is modeled by a coherent initial state of amplitude α_2. The two fields in port 1 and 2 are mixed via beam-splitter transformation, resulting in the fields in ports 3 and 4 (see Fig. 4 in the case where the emitter is a cavity).

We first derive the evolution of the emitter's state associated with detecting a number n_3 of photons (n_4) photons at port 3 (4), which is encoded in operator $M(n_3, n_4)$:

$$M(n_3, n_4) = {}_4\langle n_4|_3\langle n_3|\hat{U}(\Delta t)|0\rangle_1|\alpha_2\rangle_2. \tag{B1}$$

Here $|n\rangle_i$ corresponds to the Fock state containing n photons at port $i \in [\![0, 4]\!]$. On the other hand the ports 1,2 are prepared in the vacuum state and a coherent state of amplitude α_2 (the local oscillator), respectively. Finally, we have denoted $\hat{U}(\Delta t)$ the joint unitary evolution of the emitter and the mode a_1, which is given up to order $O(\Delta t)$ by [70]:

$$\hat{U}(\Delta t) = \hat{\mathbb{1}} - i\Delta t\hat{H}_{\text{eff}}(0) - \sqrt{\gamma_-\Delta t}\,(\hat{a}_1^\dagger\hat{c} - \hat{a}_1\hat{c}^\dagger), \tag{B2}$$

with $\hat{H}_{\text{eff}}(0) = \hat{H}_S - i\frac{\gamma_-\Delta t}{2}\hat{c}^\dagger\hat{c}$ the NHH in the case $\beta = 0$. We have introduced $\hat{c}$ as the emitter's lowering operator, e.g., $\hat{\sigma}_-$ for a qubit, or $\hat{a}$ for a cavity, as detailed in the examples in the main text.

We can now express $\hat{a}_1$ in terms of $\hat{a}_{3,4}$ using Eq. (A2). We also express the state $|0\rangle_1|\alpha_2\rangle_2$ in the basis of the output modes, yielding the tensor product of coherent states $|\sqrt{\eta}\alpha_2\rangle_3|\sqrt{1-\eta}\alpha_2\rangle_4$. We then obtain:

$$\begin{aligned}\hat{M}(n_3, n_4) &= {}_4\langle n_4|_3\langle n_3|(\hat{\mathbb{1}} - i\Delta t\hat{H}_{\text{eff}} - \sqrt{\gamma_-\Delta t}\,(\sqrt{1-\eta}\hat{a}_3^\dagger - \sqrt{\eta}\hat{a}_4^\dagger)\hat{c})|\sqrt{\eta}\alpha_2\rangle_3|\sqrt{1-\eta}\alpha_2\rangle_4 \\ &= \langle n_3|\sqrt{\eta}\alpha_2\rangle\langle n_4|\sqrt{1-\eta}\alpha_2\rangle\left[\hat{\mathbb{1}} - i\Delta t\hat{H}_{\text{eff}}(0) - \sqrt{\gamma_-\Delta t}\left(\sqrt{1-\eta}\frac{n_3}{\sqrt{\eta}\alpha_2} - \sqrt{\eta}\frac{n_4}{\sqrt{1-\eta}\alpha_2}\right)\hat{\sigma}_-\right].\end{aligned} \tag{B3}$$

We now assume that only the photons coming from port 3 are detected. The state after a β-dyne measurement is therefore obtained by averaging over the values of n_4:

$$p(n_3)\hat{\rho}(t+\Delta t) = \sum_{n_4}\hat{M}(n_3, n_4)\hat{\rho}(t)\hat{M}^\dagger(n_3, n_4), \tag{B4}$$

where $p(n_3)$ is the probability of reading n_3 photons.

Finally we use

$$\sum_{n_4}|\langle n_4|\sqrt{1-\eta}\alpha_2\rangle|^2\sqrt{\eta}n_4 = \sqrt{1-\eta}|\alpha_2|^2, \quad \sum_{n_4}|\langle n_4|\sqrt{1-\eta}\alpha_2\rangle|^2\sqrt{\eta}n_4^2 = \sqrt{1-\eta}|\alpha_2|^2(|\alpha_2|^2+1), \tag{B5}$$

to find:

$$\begin{aligned}p(n_3)\hat{\rho}(t+\Delta t) = |\langle n_3|\sqrt{\eta}\alpha_2\rangle|^2\Bigg[&\hat{\rho}(t) - \Delta t(i\hat{H}_{\text{eff}}(0)\hat{\rho}(t) + \text{H.c.}) - \sqrt{\gamma_-\Delta t}\left(\frac{\sqrt{\eta}\alpha_2^*}{\sqrt{1-\eta}} - \frac{\sqrt{1-\eta}n_3}{\sqrt{\eta}\alpha_2}\right)\hat{c}\hat{\rho}(t) + \text{H.c.} \\ &+ \gamma_-\Delta t\left(\frac{\eta(|\alpha_2|^2+1)}{1-\eta} + \frac{(1-\eta)n_3^2}{\eta|\alpha_2|^2}\right)\hat{c}\hat{\rho}(t)\hat{c}^\dagger.\Bigg],\end{aligned} \tag{B6}$$

We now assume that η is very small (the beam-splitter transmission is almost unity) and the coherent field is intense $|\alpha_2| \gg 1$, while keeping $\sqrt{\eta}|\alpha_2$ finite. Actually, we take $\sqrt{\eta}\alpha_2 \equiv \sqrt{\gamma_-\Delta t}\beta \ll 1$. We keep only terms up to order η and $\gamma_-\Delta t$ and distinguish two measurement outcomes: $n_3 = 0$ and $n_3 > 0$. The first one is associated with backaction:

$$\begin{aligned}p(n_3 = 0)\hat{\rho}^{(0)}(t+\Delta t) &\simeq \hat{\rho}(t) + \left(-i\Delta t\left[\hat{H}_{\text{eff}}(0) - i\gamma_-\beta^*\hat{c} - i\frac{|\beta|^2\gamma_-}{2}\hat{\mathbb{1}}\right]\hat{\rho}(t) + \text{H.c.}\right) \\ &= \hat{\rho}(t) - i\Delta t\big(\hat{H}_{\text{eff}}(\beta)\hat{\rho}(t) + \hat{\rho}(t)\hat{H}_{\text{eff}}^\dagger(\beta)\big),\end{aligned} \tag{B7}$$

where

$$\hat{H}_{\text{eff}}(\beta) = \hat{H}_{\text{eff}}(0) - i\frac{\gamma_-|\beta|^2}{2}\hat{\mathbb{1}} - \gamma_-\beta^*\hat{c} \tag{B8}$$

is the β-dyne effective Hamiltonian as defined in the main text. Note that we have used that $|\langle 0|\sqrt{\eta}\alpha_2\rangle|^2 \simeq 1 - \gamma_-\Delta t|\beta|^2$.

On the other hand, the backaction associated with photon detection is obtained by summing up the terms with $n_3 > 0$:

$$p(n_3 > 0)\hat{\rho}^{(1)}(t+\Delta t) \simeq \gamma_-\Delta t|\beta|^2\hat{\rho}(t) - \left(i\Delta t\left[\hat{H}_{\text{eff}}(0) - i\gamma_-\beta^*\hat{\sigma}_- - i\frac{|\beta|^2\gamma_-}{2}\hat{\mathbb{1}}\right]\hat{\rho}(t) + \text{H.c.}\right)$$

$$+\frac{1}{\beta}\langle\langle n_3\rangle\rangle\hat{c}\hat{\rho}(t)+\text{H.c.}+\frac{1}{|\beta|^2}\langle\langle n_3^2\rangle\rangle\hat{c}\hat{\rho}(t)\hat{c}^\dagger$$
$$\simeq\gamma_-\Delta t(\hat{c}+\beta)\hat{\rho}(t)(\hat{c}+\beta^*). \tag{B9}$$

We have introduced the average $\langle\langle\cdot\rangle\rangle$ in the distribution $P(n_3)=|\langle n_3|\sqrt{\eta}\alpha_3\rangle|^2$, which verifies $\langle\langle n_3^2\rangle\rangle\simeq\langle\langle n_3\rangle\rangle=\gamma_-\Delta t|\beta|^2\ll 1$. This demonstrates that the quantum jumps associated with this detection setup are described by operator $\hat{J}_1=\hat{c}+\beta\hat{\mathbb{1}}$.

Finally, the probability of obtaining outcome $n_3=0$ is encoded in the trace of the right-hand side of equality Eq. (B7):

$$p(n_3=0)=1-\gamma_-\Delta t|\beta|^2-\Delta t\text{Tr}[i\hat{H}_{\text{eff}}(0)\hat{\rho}(t)+\text{H.c.}] \tag{B10}$$

for a single time step Δt. More generally, one therefore expects that the probability of the trajectory with no photon detection is decreased by a factor $\exp(-\gamma_-|\beta|^2t)$ with respect to the case where $\beta=0$ (direct detection of the emission).

[1] Y. Ashida, Z. Gong, and M. Ueda, Non-Hermitian physics, Adv. Phys. **69**, 249 (2020).

[2] R. El-Ganainy, K. G. Makris, M. Khajavikhan, Z. H. Musslimani, S. Rotter, and D. N. Christodoulides, Non-Hermitian physics and $\mathcal{PT}$ symmetry, Nature Phys. **14**, 11 (2018).

[3] Ş. K. Özdemir, S. Rotter, F. Nori, and L. Yang, Parity-time symmetry and exceptional points in photonics, Nature Mater. **18**, 783 (2019).

[4] T. Kato, *Perturbation Theory for Linear Operators*, Classics in Mathematics (Springer, Berlin, 1995).

[5] F. Minganti, A. Miranowicz, R. W. Chhajlany, and F. Nori, Quantum exceptional points of non-Hermitian Hamiltonians and Liouvillians: The effects of quantum jumps, Phys. Rev. A **100**, 062131 (2019).

[6] C. M. Bender and S. Boettcher, Real Spectra in Non-Hermitian Hamiltonians having $\mathcal{PT}$ Symmetry, Phys. Rev. Lett. **80**, 5243 (1998).

[7] W. D. Heiss and A. L. Sannino, Transitional regions of finite Fermi systems and quantum chaos, Phys. Rev. A **43**, 4159 (1991).

[8] Z. Lin, H. Ramezani, T. Eichelkraut, T. Kottos, H. Cao, and D. N. Christodoulides, Unidirectional Invisibility Induced by $\mathcal{PT}$-Symmetric Periodic Structures, Phys. Rev. Lett. **106**, 213901 (2011).

[9] A. Regensburger, C. Bersch, M.-A. Miri, G. Onishchukov, D. N. Christodoulides, and U. Peschel, Parity-time synthetic photonic lattices, Nature (London) **488**, 167 (2012).

[10] L. Feng, Z. J. Wong, R.-M. Ma, Y. Wang, and X. Zhang, Single-mode laser by parity-time symmetry breaking, Science **346**, 972 (2014).

[11] H. Hodaei, M.-A. Miri, M. Heinrich, D. N. Christodoulides, and M. Khajavikhan, Parity-time-symmetric microring lasers, Science **346**, 975 (2014).

[12] B. Peng, Ş. K. Özdemir, F. Lei, F. Monifi, M. Gianfreda, G. L. Long, S. Fan, F. Nori, C. Bender, and L. Yang, Parity-time-symmetric whispering-gallery microcavities, Nature Phys. **10**, 394 (2014).

[13] L. Chang, X. Jiang, S. Hua, C. Yang, J. Wen, L. Jiang, G. Li, G. Wang, and M. Xiao, Parity-time symmetry and variable optical isolation in active-passive-coupled microresonators, Nature Photon. **8**, 524 (2014).

[14] H. Jing, Ş. K. Özdemir, X.-Y. Lü, J. Zhang, L. Yang, and F. Nori, $\mathcal{PT}$-Symmetric Phonon Laser, Phys. Rev. Lett. **113**, 053604 (2014).

[15] H. Lü, Ş. K. Özdemir, L. M. Kuang, F. Nori, and H. Jing, Exceptional Points in Random-Defect Phonon Lasers, Phys. Rev. Appl. **8**, 044020 (2017).

[16] Z.-P. Liu, J. Zhang, Ş. K. Özdemir, B. Peng, H. Jing, X.-Y. Lü, C.-W. Li, L. Yang, F. Nori, and Y.-X. Liu, Metrology with $\mathcal{PT}$-Symmetric Cavities: Enhanced Sensitivity Near the $\mathcal{PT}$-Phase Transition, Phys. Rev. Lett. **117**, 110802 (2016).

[17] W. Chen, Ş. Kaya Özdemir, G. Zhao, J. Wiersig, and L. Yang, Exceptional points enhance sensing in an optical microcavity, Nature (London) **548**, 192 (2017).

[18] H. Hodaei, U. H. Absar, S. Wittek, H. Garcia-Gracia, R. El-Ganainy, D. N. Christodoulides, and M. Khajavikhan, Enhanced sensitivity at higher-order exceptional points, Nature (London) **548**, 187 (2017).

[19] M. Brandstetter, M. Liertzer, C. Deutsch, P. Klang, J. Schoberl, H. E. Tureci, G. Strasser, K. Unterrainer, and S. Rotter, Reversing the pump dependence of a laser at an exceptional point, Nature Commun. **5**, 4034 (2014).

[20] B. Peng, Ş. K. Özdemir, S. Rotter, H. Yilmaz, M. Liertzer, F. Monifi, C. M. Bender, F. Nori, and L. Yang, Loss-induced suppression and revival of lasing, Science **346**, 328 (2014).

[21] J. Schindler, A. Li, M. C. Zheng, F. M. Ellis, and T. Kottos, Experimental study of active LRC circuits with $\mathcal{PT}$ symmetries, Phys. Rev. A **84**, 040101(R) (2011).

[22] H. Xu, D. Mason, L. Jiang, and J. G. E. Harris, Topological energy transfer in an optomechanical system with exceptional points, Nature (London) **537**, 80 (2016).

[23] H. Jing, Ş. K. Özdemir, H. Lü, and F. Nori, High-order exceptional points in optomechanics, Sci. Rep. **7**, 3386 (2017).

[24] X. Zhu, H. Ramezani, C. Shi, J. Zhu, and X. Zhang, $\mathcal{PT}$-Symmetric Acoustics, Phys. Rev. X **4**, 031042 (2014).

[25] R. Fleury, D. Sounas, and A. Alù, An invisible acoustic sensor based on parity-time symmetry, Nature Commun. **6**, 5905 (2015).

[26] H. Benisty, A. Degiron, A. Lupu, A. De Lustrac, S. Chenais, S. Forget, M. Besbes, G. Barbillon, A. Bruyant, S. Blaize, and G. Lerondel, Implementation of $\mathcal{PT}$ symmetric devices using plasmonics: principle and applications, Opt. Express **19**, 18004 (2011).

[27] M. Kang, F. Liu, and J. Li, Effective spontaneous $\mathcal{PT}$-symmetry breaking in hybridized metamaterials, Phys. Rev. A **87**, 053824 (2013).

[28] D. Leykam, K. Y. Bliokh, C. Huang, Y. D. Chong, and F. Nori, Edge Modes, Degeneracies, and Topological Numbers in Non-Hermitian Systems, Phys. Rev. Lett. **118**, 040401 (2017).

[29] J. González and R. A. Molina, Topological protection from exceptional points in Weyl and nodal-line semimetals, Phys. Rev. B **96**, 045437 (2017).

[30] W. Hu, H. Wang, P. P. Shum, and Y. D. Chong, Exceptional points in a non-Hermitian topological pump, Phys. Rev. B **95**, 184306 (2017).

[31] T. Gao, G. Li, E. Estrecho, T. C. H. Liew, D. Comber-Todd, A. Nalitov, M. Steger, K. West, L. Pfeiffer, D. W. Snoke, A. V. Kavokin, A. G. Truscott, and E. A. Ostrovskaya, Chiral Modes at Exceptional Points in Exciton-Polariton Quantum Fluids, Phys. Rev. Lett. **120**, 065301 (2018).

[32] T. Liu, Y.-R. Zhang, Q. Ai, Z. Gong, K. Kawabata, M. Ueda, and F. Nori, Second-Order Topological Phases in Non-Hermitian Systems, Phys. Rev. Lett. **122**, 076801 (2019).

[33] L. Zhou, Q.-H. Wang, H. Wang, and J. Gong, Dynamical quantum phase transitions in non-Hermitian lattices, Phys. Rev. A **98**, 022129 (2018).

[34] K. Y. Bliokh, D. Leykam, M. Lein, and F. Nori, Topological non-Hermitian origin of surface Maxwell waves, Nature Commun. **10**, 580 (2019).

[35] M. van Caspel, S. E. T. Arze, and I. P. Castillo, Dynamical signatures of topological order in the driven-dissipative Kitaev chain, SciPost Phys. **6**, 026 (2019).

[36] Z.-Y. Ge, Y.-R. Zhang, T. Liu, S.-W. Li, H. Fan, and F. Nori, Topological band theory for non-Hermitian systems from the Dirac equation, Phys. Rev. B **100**, 054105 (2019).

[37] T. Yoshida, R. Peters, N. Kawakami, and Y. Hatsugai, Symmetry-protected exceptional rings in two-dimensional correlated systems with chiral symmetry, Phys. Rev. B **99**, 121101(R) (2019).

[38] Z. Gong, Y. Ashida, K. Kawabata, K. Takasan, S. Higashikawa, and M. Ueda, Topological Phases of Non-Hermitian Systems, Phys. Rev. X **8**, 031079 (2018).

[39] K. Kawabata, K. Shiozaki, M. Ueda, and M. Sato, Symmetry and Topology in Non-Hermitian Physics, Phys. Rev. X **9**, 041015 (2019).

[40] A. McDonald, R. Hanai, and A. A. Clerk, Phys. Rev. B **105**, 064302 (2022).

[41] W. Nie, M. Antezza, Y.-X. Liu, and F. Nori, Dissipative Topological Phase Transition with Strong System-Environment Coupling, Phys. Rev. Lett. **127**, 250402 (2021).

[42] E. J. Bergholtz, J. C. Budich, and F. K. Kunst, Exceptional topology of non-Hermitian systems, Rev. Mod. Phys. **93**, 015005 (2021).

[43] I. I. Arkhipov and F. Minganti, Emergent non-Hermitian skin effect in the synthetic space of (anti-) PT-symmetric dimers, arXiv:2110.15286 (2021).

[44] M. Miri and A. Alù, Exceptional points in optics and photonics, Science **363**, eaar7709 (2019).

[45] L. Feng, R. El-Ganainy, and L. Ge, Non-Hermitian photonics based on parity-time symmetry, Nature Photon. **11**, 752 (2017).

[46] H.-K. Lau and A. A. Clerk, Fundamental limits and non-reciprocal approaches in non-Hermitian quantum sensing, Nature Commun. **9**, 4320 (2018).

[47] W. Langbein, No exceptional precision of exceptional-point sensors, Phys. Rev. A **98**, 023805 (2018).

[48] M. Zhang, W. Sweeney, C. W. Hsu, L. Yang, A. D. Stone, and L. Jiang, Quantum Noise Theory of Exceptional Point Amplifying Sensors, Phys. Rev. Lett. **123**, 180501 (2019).

[49] F. Minganti, A. Miranowicz, R. W. Chhajlany, I. I. Arkhipov, and F. Nori, Hybrid-Liouvillian formalism connecting exceptional points of non-Hermitian Hamiltonians and Liouvillians via postselection of quantum trajectories, Phys. Rev. A **101**, 062112 (2020).

[50] M. H. Teimourpour, R. El-Ganainy, A. Eisfeld, A. Szameit, and D. N. Christodoulides, Light transport in $\mathcal{PT}$-invariant photonic structures with hidden symmetries, Phys. Rev. A **90**, 053817 (2014).

[51] Y. Wu, W. Liu, J. Geng, X. Song, X. Ye, C.-K. Duan, X. Rong, and J. Du, Observation of parity-time symmetry breaking in a single-spin system, Science **364**, 878 (2019).

[52] M. Naghiloo, M. Abbasi, Y. N. Joglekar, and K. W. Murch, Quantum state tomography across the exceptional point in a single dissipative qubit, Nature Phys. **15**, 1232 (2019).

[53] W. Chen, M. Abbasi, Y. N. Joglekar, and K. W. Murch, Quantum Jumps in the Non-Hermitian Dynamics of a Superconducting Qubit, Phys. Rev. Lett. **127**, 140504 (2021).

[54] P. Kwiat, H. Weinfurter, T. Herzog, A. Zeilinger, and M. A. Kasevich, Interaction-Free Measurement, Phys. Rev. Lett. **74**, 4763 (1995).

[55] P. Campagne-Ibarcq, L. Bretheau, E. Flurin, A. Auffèves, F. Mallet, and B. Huard, Observing Interferences between Past and Future Quantum States in Resonance Fluorescence, Phys. Rev. Lett. **112**, 180402 (2014).

[56] H. P. Breuer and F. Petruccione, *The Theory of Open Quantum Systems* (Oxford University Press, Oxford, 2007).

[57] D. F. Walls and G. J. Milburn, *Quantum Optics* (Springer, Berlin, 2011).

[58] K. Mølmer, Y. Castin, and J. Dalibard, Monte Carlo wave-function method in quantum optics, J. Opt. Soc. Am. B **10**, 524 (1993).

[59] J. Dalibard, Y. Castin, and K. Mølmer, Wave-Function Approach to Dissipative Processes in Quantum Optics, Phys. Rev. Lett. **68**, 580 (1992).

[60] S. Haroche and J. M. Raimond, *Exploring the Quantum: Atoms, Cavities, and Photons* (Oxford University Press, Oxford, 2006).

[61] N. Bartolo, F. Minganti, J. Lolli, and C. Ciuti, Homodyne versus photon-counting quantum trajectories for dissipative kerr resonators with two-photon driving, Eur. Phys. J.: Spec. Top. **226**, 2705 (2017).

[62] R. Rota, F. Minganti, A. Biella, and C. Ciuti, Dynamical properties of dissipative xyz heisenberg lattices, New J. Phys. **20**, 045003 (2018).

[63] C. Sánchez Muñoz, B. Buča, J. Tindall, A. González-Tudela, D. Jaksch, and D. Porras, Symmetries and conservation laws in quantum trajectories: Dissipative freezing, Phys. Rev. A **100**, 042113 (2019).

[64] P. Campagne-Ibarcq, P. Six, L. Bretheau, A. Sarlette, M. Mirrahimi, P. Rouchon, and B. Huard, Observing Quantum State Diffusion by Heterodyne Detection of Fluorescence, Phys. Rev. X **6**, 011002 (2016).

[65] H. M. Wiseman and G. J. Milburn, *Quantum Measurement and Control* (Cambridge University Press, Cambridge, 2009).

[66] A. R. R. Carvalho and M. F. Santos, Distant entanglement protected through artificially increased local temperature, New J. Phys. **13**, 013010 (2011).

[67] M. F. Santos and A. R. R. Carvalho, Observing different quantum trajectories in cavity QED, Europhys. Lett. **94**, 64003 (2011).

[68] S. Assawaworrarit, X. Yu, and S. Fan, Robust wireless power transfer using a nonlinear parity–time-symmetric circuit, Nature (London) **546**, 387 (2017).

[69] S. Khandelwal, N. Brunner, and G. Haack, PRX Quantum **2**, 040346 (2021).

[70] P. Lewalle, S. K. Manikandan, C. Elouard, and A. N. Jordan, Measuring fluorescence to track a quantum emitter's state: a theory review, Contemp. Phys. **61**, 26 (2020).